Received: 27 November 2019 | Revised: 18 January 2020 | Accepted: 20 January 2020

DOI: 10.1002/prp2.565

ORIGINAL ARTICLE

ZYBT1, a potent, irreversible Bruton's Tyrosine Kinase (BTK) inhibitor that inhibits the C481S BTK with profound efficacy against arthritis and cancer

Krishnarup Ghoshdastidar[1] | Hoshang Patel[1] | Hitesh Bhayani[1] | Ankit Patel[1] | Kinjal Thakkar[1] | Dinesh Patel[2] | Manoranjan Sharma[2] | Jaideep Singh[2] | Jogeswar Mohapatra[2] | Abhijit Chatterjee[2] | Dipam Patel[3] | Rajesh Bahekar[3] | Rajiv Sharma[3] | Lakshmikant Gupta[4] | Nirmal Patel[4] | Poonam Giri[4] | Nuggehally R. Srinivas[4] | Mukul Jain[5] | Debdutta Bandyopadhyay[1] | Pankaj R. Patel[6] | Ranjit C. Desai[3]

[1]Department of Cell Biology, Zydus Research Center, Ahmedabad, Gujarat, India

[2]Department of Pharmacology, Zydus Research Center, Ahmedabad, Gujarat, India

[3]Department of Medicinal Chemistry, Zydus Research Center, Ahmedabad, Gujarat, India

[4]Department of Pharmacokinetics, Zydus Research Center, Ahmedabad, Gujarat, India

[5]Department of Pharmacology and Toxicology, Zydus Research Center, Ahmedabad, Gujarat, India

[6]Zydus Research Center, Ahmedabad, Gujarat, India

Correspondence
Debdutta Bandyopadhyay, Zydus Research Centre, Sarkhej-Bavla, NH 8A, Moraiya, Ahmedabad, Gujarat, India 382210.
Email: debduttabandyopadhyay@zyduscadila.com

Abstract

Bruton's tyrosine kinase (BTK) plays a central and pivotal role in controlling the pathways involved in the pathobiology of cancer, rheumatoid arthritis (RA), and other autoimmune disorders. ZYBT1 is a potent, irreversible, specific BTK inhibitor that inhibits the ibrutinib-resistant C481S BTK with nanomolar potency. ZYBT1 is found to be a promising molecule to treat both cancer and RA. In the present report we profiled the molecule for in-vitro, in-vivo activity, and pharmacokinetic properties. ZYBT1 inhibits BTK and C481S BTK with an IC_{50} of 1 nmol/L and 14 nmol/L, respectively, inhibits the growth of various leukemic cell lines with IC_{50} of 1 nmol/L to 15 μmol/L, blocks the phosphorylation of BTK and PLCγ2, and inhibits secretion of TNF-α, IL-8 and IL-6. It has favorable pharmacokinetic properties suitable for using as an oral anti-cancer and anti-arthritic drug. In accordance with the in-vitro properties, it demonstrated robust efficacy in murine models of collagen-induced arthritis (CIA) and streptococcal cell wall (SCW) induced arthritis. In both models, ZYBT1 alone could suppress the progression of the diseases. It also reduced the growth of TMD8 xenograft tumor. The results suggested that ZYBT1 has high potential for treating RA, and cancer.

KEYWORDS

Bruton's tyrosine kinase, cancer, irreversible inhibitor, rheumatoid arthritis, xenograft

Abbreviations: BCR, B-cell receptor; BTK, Bruton's tyrosine kinase; CAIA, collagen antibody-induced arthritis; CIA, collagen-induced arthritis; DLBCL, diffused large B-cell lymphoma; GCB-DLBCL, germinal center B-cell diffused large B-cell lymphoma; IB-BFL, BODIPY-labeled Ibrutinib; MCL, mantle cell lymphoma; Papp, apparent permeability; pBTK, phospho-BTK; PGPS, peptidoglycanpolysaccharide; TNFAIP3, Tumor necrosis factor, alpha-induced protein 3; WM, Waldenstrom's Macroglobulinemia; XLA, X-linked Bruton's agammaglobulinemia.

1 | INTRODUCTION

B-cell receptor (BCR) signaling pathway plays a major role in the development of B-cells. Starting from the precursor state in bone marrow to its fully matured plasma-B cells or memory B-cell subpopulation, a highly regulated and concerted mechanism is in effect. However, disruption of this mechanism at various states of B-cell maturation scheme may lead to various kinds of B-cell malignancies. For example, a naïve B-cell can give rise to mantle cell lymphoma (MCL), while an antigen-experienced B cell can give rise to chronic lymphocytic lymphoma (CLL) or small lymphocytic lymphoma (SLL). On the other hand, diffused large B-cell lymphoma (DLBCL) arises from deleterious mutations incurred during the somatic hyper-mutation step in lymph node.[1] Bruton's tyrosine kinase (BTK) is one of the key enzymes of the BCR pathway. Post the initiation of the BCR signaling, BTK phosphoryates and activates phospholipase C gamma2 (PLCγ2), which in turn activates NFκ-b.[2] Mutation of BTK was first noted in patients with X-linked Bruton's agammaglobulinemia (XLA).[3] Further instances of involvement of BTK in CLL, MCL, DLBCL, and other types of lymphoma[4] have made it a lucrative target for treatment of cancer.

Since BCR signaling is important for normal development of B-cells, BTK has been shown to play key role in several auto-immune disorders like lupus, rheumatoid arthritis, multiple sclerosis, and others.[5,6] The presence of abnormal B cell and autoantibodies in most RA patients, primarily ACPA and RF, indicates that the function of B cell was involved in the development of RA disease.[7] Similarly, BTK has also been implicated as one of the potential targets for treating multiple sclerosis (MS). In fact, PRN2246, a BTK inhibitor, being developed for MS has completed Phase I trials.

Moreover, BTK has been shown to function in Toll-like receptors-mediated recognition of infectious agents and Fc receptor signaling. Of these two, Fc receptor signaling is of special importance in BTK signaling. Immune cells like mast cell, basophils, monocytes, macrophages play important roles in inflammatory and allergic responses. These responses are believed to be initiated partly by cross-linking of the high affinity receptor for IgE (FcεRI) on these cells.[8] This activates intracellular signaling pathways leading to degranulation and release of histamine and other pro-inflammatory cytokines. Constitutive BTK activation under autoimmune condition, therefore, leads to activation of FcεRI. In addition to that, Fcγ receptors (FcγR) on immune cells such as macrophages also play an important role in tumor-specific antibody-mediated immune responses involving BTK.[9] Recently, BTK is found as a direct regulator of NLRP3 inflammasome.[10]

Among the BTK inhibitors, ibrutinib, acalabrutinib, and zanubrutinib are currently approved various authorities. Furthermore, ibrutinib has also been approved for patients with marginal zone lymphoma (MZL), who require systemic therapy and have received at least one prior anti-CD20-based therapy.

Here, we report the discovery and preclinical profiling of ZYBT1, a novel, irreversible covalent BTK inhibitor, that has demonstrated in-vitro potency toward both wild-type and C481S mutant BTK and efficacious in animal models of Streptococcus cell wall mediated and collagen induced arthritis as well as B-cell lymphoma.

2 | MATERIALS AND METHODS

2.1 | Reagents and cell culture

ZYBT1, ibrutinib, dasatinib, and acalabrutinib and BODIPY-labeled ibrutinib (IB-BFL) were synthesized in house, at the Department of Medicinal Chemistry (Zydus Research Centre, Cadila Healthcare Ltd, Ahmedabad). Purified recombinant human BTK (wild-type) and mutant BTK (C481S) were purchased from SignalChem, USA. ADP-Glo reagent assay was from Promega Corp, USA. TMD8, HBL-1, U2932, SUDHL6, JEKO, MINO were kind gift from Richard Eric Davis, MD Anderson Cancer Center, Houston, TX. Raji and THP1 were obtained from ATCC. Cells were routinely grown and treated at 37°C and 5% CO2 in humidified incubator, unless otherwise mentioned. All cell culture media, supplements, antibiotics, trypsin from porcine pancreas, EDTA, Tween 20, MTT powder, Poly Glu:Tyr (4:1), and Human IgG were purchased from Sigma-Aldrich. Human phospho-BTK (Y223) antibody and human BTK antibody were from R&D system. Human phospho-PLCγ2 (Y1217) and human PLCγ2 rabbit polyclonal antibody, human TNFα, IL-6 and IL-8 ELISA kits were purchased from Mabtech AB, Sweden. All animal care and experimental procedures were in compliance with the guidelines of the Committee for the Purpose of Control and Supervision of Experiments on Animals (CPCSEA) as stated by the National Institutes of Health and were approved by the Institutional Animal Ethics Committee (IAEC). Studies were conducted in an Association for Assessment and Accreditation of Laboratory Animal Care (AAALAC) International accredited facility. Six to eight weeks old SCID mice were used for the in vivo xenograft studies.

2.2 | Chemical synthesis of ZYBT1

Synthetically, ZYBT1 [4-(1-(2-acryloyloctahydrocyclopenta[c]pyrrol-5-yl)-4-amino-1H-pyrazolo[3,4-d]pyrimidin-3-yl)-N-(pyridin-2-yl) benzamide] was prepared in a step wise manner as described elsewhere.[11] Initially Mitsunobu reaction of 3-iodo-1H-pyrazolo[3,4-d]pyrimidin-4-amine nucleophile was carried out with tert-butyl 5-hydroxyhexahydrocyclopenta[c]pyrrole-2(1H)-carboxylate derived from Hexahydrocyclopentapyrrolone[12] to give tert-butyl 5-(4-amino-3-iodo-1H-pyrazolo[3,4-d]pyrimidin-1-yl)hexahydrocyclopenta[c] pyrrole-2(1H)-carboxylate. Product thus obtained was coupled with (4-(pyridin-2-ylcarbamoyl)phenyl) boronic acid via palladium-catalyzed Suzuki-Miyaura coupling reaction which upon Boc group de-protection using trifluoroacetic acid followed by acylation with acrolyl chloride provided ZYBT1 with good yield and purity.

^{1}H NMR: ($CDCl_3$, 400 MHz): δ 8.72 (s, 1H), 8.43 (d, 1H, *J* = 6.4 Hz), 8.39 (s, 1H), 8.35-8.34 (m, 1H), 8.13 (d, 2H, *J* = 8.4 Hz), 7.88 (d,

2H, J = 8.4 Hz), 7.83-7.79 (m, 1H), 7.14-7.11 (m, 1H), 6.49 (dd, 1H, J_1 = 10.0 Hz, J_2 = 16.8 Hz), 6.42 (dd, 1H, J_1 = 2.4 Hz, J_2 = 16.8 Hz), 5.72 (dd, 1H, J_1 = 2.8 Hz, J_2 = 10.0 Hz), 5.61-5.55 (m, 3H), 3.89-3.84 (m, 2H), 3.57-3.47 (m, 2H), 3.24-3.21 (m, 1H), 315-3.12 (m, 1H), 2.60-2.52 (m, 2H), 2.21-2.14 (m, 1H); ESI-MS: (+ve mode) 495.4 $(M + H)^+$ (100%); HPLC: 99.09%, Ret.time = 11.92 minutes.

2.3 | BTK enzyme activity assay

The enzymatic activity of ZYBT1 was assessed in a cell-free enzyme assay. Briefly, fixed amount of recombinant purified human BTK-WT (3 ng/reaction) or BTK-C418S (20 ng/reaction) was incubated with increasing concentration of ZYBT1 (0.01 nmol/L to 10 µmol/L) in 1X kinase reaction buffer (40 mmol/L Tris-Cl, pH7.5, 20 mmol/L $MgCl_2$, 2 mmol/L $MnCl_2$, 0.1 mg/ml BSA and 50 µmol/L DTT). Enzymatic reaction was initiated by adding a substrate cocktail containing 50 µmol/L of ATP (final concentration) and 5 µg of $polyGln_4Tyr_1$ in total 25 µL of reaction in round bottom white 96 well plates. The reaction was incubated at room temperature for 2 hours followed by quantification of the left over ATP according to the manufacturer's protocol using ADP-Glo reagent. Data were plotted taking 'enzyme with no inhibitor' as the 100% kinase activity.

For determining the Ki, Omnia Tyr peptide kit was used and the protocol supplied by the manufacturer was followed. Briefly, 10 nmol/L BTK-WT enzyme was incubated with increasing concentration of ZYBT1 (0.5 nmol/L to 1.0 µmol/L) and a mixture of substrate (ATP and 8-hydroxy-5-(N, N-dimethylsulfonamido)-2-methylquinoline, referred to as SOX). The reaction mixture was incubated at 25°C for 3 hours and fluorescence intensity was read at predetermined interval of 30 seconds in Tecan Infinite M1000 PRO using excitation and emission wave lengths of 360 nm and 485 nm respectively. Data were plotted taking "No inhibitor" control set as the 100% kinase activity. The obtained net progress curves were then fitted according to an ascending single-exponential Equation[13] to yield k_{obs} values at each compound concentration using GraphPad Prism software version 8.0. Plots of k_{obs} vs [Inhibitor] were fitted according to a simplified version of the hyperbola equation (for [substrate]«Km) suggested by Evans, to generate apparent kinetics and Ki values.

The Kinase profiling for ZYBT1 for addressing its selectivity was done from ProQuinase (GmbH). A radiometric protein kinase assay was used in 96 well FlashPlates™ from Perkin Elmer.

2.4 | Cell cytotoxicity assay

TMD8, HBL-1, U2932, SUDHL6, JEKO, MINO, Raji cells were routinely grown in RPMI-1640 with 10% FBS and supplemented with 55 µmol/L β-mercapto ethanol (β-ME). For cytotoxicity assay, defined numbers of cells were incubated in 96 well plates with increasing concentration of ZYBT1, formulated in 100% DMSO (final concentration of DMSO in the well is 0.2%) for 96 hours. Cell growth was measured using MTT assay and IC_{50} values were determined by nonlinear regression using the GraphPad Prism 6 software. For drug wash out experiments, TMD8 cells were treated with ZYBT1 (25 nmol/L), ibrutinib (25 nmol/L) and dasatinib (100 nmol/L) for 5 hours, cells were washed with sterile PBS thrice and were further grown for 24 and 48 hours in complete medium. Finally, cell viability was measured by MTT assay.

2.5 | Fluorescence binding assay

Florescent binding assay was performed following a protocol as described elsewhere.[14] To determine saturation binding concentration of IB-BFL for BTK, THP-1 cells were incubated with increasing concentration of IB-BFL in 96 well plates in dark. The cells were washed, lysed in SDS-PAGE loading dye and analyzed by SDS-PAGE and fluorescent gel scanning using BioRad ChemiDoc MP (using blue laser).

To determine receptor occupancy, THP-1 cells were treated with different concentrations of ZYBT1 for 1 hour followed by labeling the cells with 2 µmol/L of IB-BFL for another 1 hour in dark. Cells were washed, lysed in SDS-PAGE loading dye and finally analyzed by SDS-PAGE and fluorescent gel scanning using ChemiDoc MP imaging system, BioRad (using blue laser). As a loading control, total cellular BTK level was measured by western blot using human anti-BTK antibody.

To determine the receptor residence time, THP-1 cells, grown in two separate sets, were treated with a fixed concentration (500 nmol/L) of ZYBT1 for 1 hour and then washed three times with sterile PBS. In one set, IB-BFL (2 µmol/L) was added for 1 hour in dark (T_0 hr) while the other set was further grown for another 24 hours in complete medium followed by labeling with IB-BFL (for 1 hour) and finally treated cells from both the sets were washed, lysed in SDS-PAGE loading dye and analyzed by SDS/PAGE and fluorescent gel scanning. Similarly, total BTK control was also run in this case. For quantification, band intensities were assessed by densitometric scanning. The percentage of IB-BFL, bound to BTK was calculated after normalization with total cellular BTK level against concentration of ZYBT1 using GraphPad Prism 6.0 software.

2.6 | Cell washout

Approximately, 1×10^4 TMD8 cells/well were seeded in Poly L-Lysine coated 96-well cell culture plate and incubated overnight at 37°C/5% CO_2 humidified incubator. Next day, drug treatment was carried out for 5 hours in both "washout" and "no washout" sets. In the washout condition, inhibitor containing growth media was replaced with fresh media and cells were allowed to grow for 24 hours and 48 hours. Finally, cell proliferation was measured by MTT assay for both the time points.

2.7 | Phospho-protein analysis

To determine the effect of ZYBT1 on phosphorylation of BTK and PLCγ2, THP-1 cells were treated with increasing concentration of ZYBT1 for 1 hour followed by a brief pervanadate (500 µmol/L final concentration) treatment for 10 minutes in 96 well plates. The cells were washed thrice with ice cold sterile PBS, lysed in SDS-PAGE loading dye and analyzed by western blot using human anti-phospho-BTK (Y223) antibody or human phospho-PLCγ2 (Y1217) antibody. For total cellular BTK and PLCγ2, blots were stripped and re-probed with human anti-BTK antibody or human anti-PLCγ2 antibody. To determine receptor resident time, T_0 and T_{24} sets were prepared as described above, only with the exception that in this case no labeled compound were added and cells were lysed after the stipulated time and analyzed in SDS-PAGE and immunoblotting.

2.8 | Cytokine ELISA

Approximately 2 × 10^5 THP-1 (for TNF-α) cells/well were treated with increasing concentration of ZYBT1 (0.2 nmol/L to 40 µmol/L) in 96 well plate for 1 hour Then cells were transferred to a 96 well plate precoated with 100 µg/well human IgG (Sigma) and incubated for another 4 hours. Culture supernatants from the respective wells were collected and analyzed for secreted TNFα using human TNF-α ELISA kit. For IL-6 and IL-8 secretion assay, approximately 3 × 10^5 TMD8 cells/well were treated with increasing concentrations of ZYBT1 (0.02 nmol/L to 20 µmol/L) in 96 well plate for 16 hours and culture supernatants from the respective wells were collected and analyzed for secreted IL-6 or IL-8 using human IL-6 or IL-8 ELISA kit respectively.

2.9 | In vitro/In vivo pharmacokinetic evaluation

Permeability/efflux ratio of ZYBT1 was determined using the system comprising of the Caco-2 cell monolayers with prespecified tier values. Caco-2 cells were seeded onto 24 well filter membranes and cultured for 21 days to achieve the required specifications. Following in vitro incubation of 2 µmol/L ZYBT1 at 37°C, 95% relative humidity, 5% CO_2, samples were collected from both apical and basal side and analyzed.

In vitro metabolism was determined by incubating ZYBT1 at 1 µmol/L (37°C, 100 rpm) with liver microsomes (0.5 mg/mL) from mouse, rat, dog, monkey, and human, in the presence of NADPH (1 mmol/L) for 30 minutes in triplicate. The zero minute samples were made in the absence of NADPH and were used as control. The metabolic stability (% remaining of ZYBT1) in incubated samples was assessed with respect to 0 minutes control samples. In vitro CYP inhibition was performed by incubation of ZYBT1 at 0.1, 0.3, 1, 3, 10, 30, and 100 µmol/L with human liver microsomes and NADPH in the presence of CYP-specific substrates.

In vivo pharmacokinetics/ bioavailability studies of ZYBT1 were performed in male or female mice, and rats, using parallel study design (n = 3 to 5 per group). The oral dose was administered via gavage under overnight fasted condition and intravenous dose was administered as a bolus via tail vein injection under nonfasted condition. An aqueous suspension of ZYBT1 was used for oral dosing. The intravenous solution was prepared in 10% NMP, 5% ethanol, and 85% citric acid in purified water. Blood samples were collected serially from each animal at 0 hour, (pre-dose), and 0.08 (IV only) 0.25, 0.5, 1, 2, 4, 6, 8, 24, 48, and 72 hours post-dose. The blood samples were centrifuged (3 220 *g* for 15 minutes) to obtain plasma samples which were stored frozen in labeled tubes at or below −70°C until analysis. Pharmacokinetic parameters were derived using the noncompartmental analysis (NCA) module of WinNonlin® software.

The pharmacokinetics of ZYBT1 was evaluated in male BALB/c mice and male Wistar rats by single oral (3 mg/kg) and intravenous (1 mg/kg) routes of drug administration. All animals were quarantined in the animal house of Zydus Research Centre for a 7 days period with 12 hour dark/light cycle. During this period the animals had free access to standard pellet feed and water ad libitum. The experiment protocols were approved by the Committee for the Purpose of Control and Supervision of Experimentation on Animals (CPCSEA), Government of India and Institutional Animal Ethics Committee (IAEC), Zydus Research Centre.

The animals (male BALB/c mice (7-12 week age, 30-35 g body weight, 12 animals/route, maximum 3 blood collection/mouse, sparse sampling) and male Wistar rats (7-12 week age, 200-250 g body weight, 4 animals/route, serial blood collection) were overnight fasted before the oral gavage dosing of ZYBT1 but were given access to water ad libitum; however, food was provided 4 hour after dosing. The intravenous dosing in either mice or rats was carried out with a solution formulation, prepared in 10% NMP, 5% ethanol and 85% of 0.1% citric acid in purified water. The oral dosing in either mice or rats was performed by a homogenous suspension formulation, prepared in 1% Tween- 80 and 0.5% methyl cellulose in purified water. Blood samples either in mice or rats were collected at 0.08 (iv only), 0.25, 0.5, 1, 2, 4, 6, 8, and 24 hour post-dose in Na-heparin coated microcentrifuge tubes. Blood samples were centrifuged to separate plasma which were then stored at −70°C until analysis.

2.10 | Measurement of ZYBT1 in plasma samples

Stock and working solutions of ZYBT1 for calibration curve (CC) standards and quality control (QC) samples were prepared in acetonitrile: purified water (80:20, v/v). All primary stock and working solutions were stored at 2-8°C. The individual CCs were freshly prepared on the day of the analysis with a maximum of 10% spiking of the appropriate working solution to the respective control plasma, followed by addition of alprazolam, which served as internal standards (IS).

An HPLC system (Shimadzu, Kyoto, Japan) coupled with MDS SCIEX API 3000 mass spectrometer (MDS SCIEX, Concord Ontario, Canada) and SIL-HTc auto sampler (maintained at 10°C) was used for quantitative analysis of ZYBT1. The mass spectrometer was equipped with a Turbo ion spray interface at 600°C using a positive ion mode. The analytical column was, ACE C18, 50 × 4.6 mm, 5 µm (ACE, Scotland) and gradient elution was employed for chromatographic separation of analyte and IS from endogenous plasma matrix; mobile phases comprising of an aqueous (A) 0.065 mmol/L ammonium acetate a in purified water containing 0.01% TFA (trifluoroacetic acid) (B) acetonitrile and (C) mixture of isopropyl alcohol: methanol: purified water (40:40:20, v/v/v). The retention times of ZYBT1 and IS were about 1.5 and 1.7 minutes, respectively. The mass spectrometer was equipped with a Turbo ion spray interface at 600°C using a positive ion mode. The multiple reaction mode (MRM) parameters for the mass spectrometry detection were optimized; a multiple mass transition pairs used were (m/z 432.2 to 390.0; m/z 432.2 to 281; m/z 432.2 to 123.1; m/z 432.2 to 153.1) were used for ZYBT1 and a single transition pair of m/z 309.0 to 281.0 was used for IS.

A 50 µL of study samples obtained from mice and rats were transferred into a 2 mL micro centrifuge tube. Six µL of working solution of IS (2.0 µg/mL) was added followed by vortex-mix for 30 sec. Acetonitrile (300 µL) was added to each sample and vortexed for 1 minutes. Samples were then centrifuged at 11 200 *g* for 5 minutes and the clear supernatant was transferred to vials for LC-MS/MS analysis. The calibration curve ranging from 1 to 1000 ng/ml (with a lower limit of quantitation 1 ng/mL) was employed for quantitation of ZYBT1. The analytical data were processed using Analyst Software version 1.6.2 (MDS SCIEX, Concord Ontario, Canada).

2.11 | TMD-8 xenograft model

The xenograft studies were conducted in 6-8-week-old SCID mice. A total of 10×10^6 TMD-8 cells was suspended in 200 µL of phosphate buffer saline and subcutaneously injected into the flank. When tumors were palpable, animals were grouped so that the average tumor volume was around 100 mm^3. They were assigned to four groups: vehicle and three groups for ZYBT1 treatment (1.5, 3 & 15 mg/kg, BID) and treatment was continued for 20 days. The length and width of the tumor were measured using a digital caliper, and the volume of the tumor was calculated using the formula: length × $(width)^2/2$.

2.12 | Collagen-induced arthritis in mice

DBA1/J male mice, 8-10 weeks old, were immunized on day 0 and 21 for induction of arthritis with bovine type II collagen via intradermal injection at the base of the tail. Injection volumes were 0.1 ml aliquots, consisting of a 1:1 (vol:vol) emulsion of *Mycobacterium tuberculosis* (2 mg/mL in mineral oil) and bovine type II collagen (2 mg/ml in 10 mmol/L acetic acid). ZYBT1 was administered orally once a day for 4 weeks. Clinical scores, an index of arthritis, were assessed according to Scales HE et al[15] by using the following criteria: 0, normal with no swelling or redness; 1, swelling and/or redness of paw or one joint; 2, swelling in two or more joints; 3, gross swelling of paw with more than two joints involved; and 4, severe arthritis of entire paw and joints.

2.13 | Streptococcal cell wall (SCW) induced arthritis

Rats were primed with an intra-articular injection of 20 µL of PGPS in 0.5 mg/ml of rhamnose in the right ankle. At 2 weeks, the paw volume were measured with UGO Basile plethysmometer and rats were assigned to groups of n = 9 to get a similar distribution of initial joint paw volume. Rats then received their first dose of ZYBT1 and an iv injection of 0.5 ml of PGPS (1 hour post-ZYBT1 administration) via the tail vein. One hour later blood was collected for IL-6 measurement using a commercially available rat IL-6 ELISA kit. ZYBT1 was dosed once daily (OD) and paw volume and body weights were measured for three consecutive days.

2.14 | Statistical analysis

Data are expressed as mean ± SEM of three individual experiments unless otherwise mentioned. The statistical analysis was performed using one-way ANOVA followed by Dunnett's test used for comparison of all the parameters between treatment and control groups. For each analysis, *P*-values less than .05 were considered to be statistically significant. All analyses were performed using GraphPad Prism software (GraphPad, La Jolla, CA, USA).

3 | RESULTS

3.1 | Characterization of ZYBT1

The structure of ZYBT1 is shown in Figure 1. After purification through HPLC, the purity was found to be 99.09% with a retention time of 11.92 minutes.

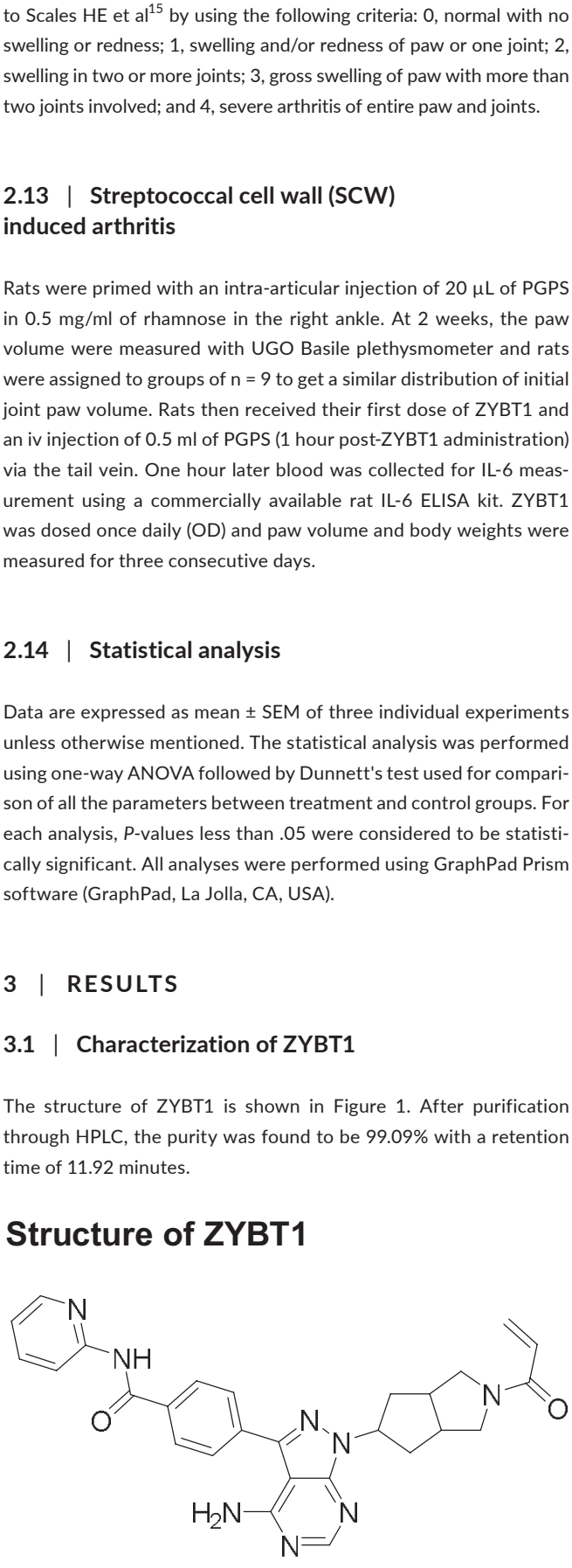

FIGURE 1 Structure of ZYBT1

TABLE 1 In vitro potency of ZYBT1 against BTK wild-type and mutant enzymes. In a cell free system the IC_{50} and the Ki (range found from three independent experiments) were measured and tabulated

Enzyme	Parameter
BTK-WT	IC_{50}: 1-2 nmol/L
BTK-WT	K_i: 14-19 nmol/L
BTK (C418S)	IC_{50}: 12-17 nmol/L

3.2 | ZYBT1 is a potent and selective inhibitor of BTK

With the aim of using BTK as a target for leukemia and inflammatory disorders, we screened a series of compounds and identified ZYBT1 as a novel, potent, selective, and irreversible BTK inhibitor. Structurally, it is a pyrazolo[3,4-d]pyrimidinyl derivative having acryloyl group, which has been specifically incorporated to interact covalently with BTK in order to retain the irreversible BTK inhibitory activity. ZYBT1 has potent inhibitory activity for wild-type as well as C481S mutant of BTK with IC_{50} values of 1 and 14 nmol/L respectively (Table 1). The dissociation constant, Ki of ZYBT1 for wt BTK was found to be 14 nmol/L indicative of a strong binding (Table 1). Screening of a panel of other 13 different kinases demonstrated that ZYBT1 is highly selective for BTK and TEC, while for other tyrosine kinases namely EGFR, ERB, and JAK, ZYBT1 is >1000 times less potent (Table 2).

3.3 | ZYBT1 inhibits a battery of cell lines representing various leukemia subtypes

In order to predict the efficacy of ZYBT1 in various leukemia populations, we tested the potency of this compound in a series of cell lines that represents leukemia subtypes. These include TMD-8, HBL-1, U2932 (representing ABC-DLBCL subtype), SUDHL6 (GCB-DLBCL), JEKO (MCL) and Raji (Burkitt's lymphoma). The cell killing potency (IC_{50}) varied from 1 nmol/L (in TMD-8) to 15 μmol/L (in Raji) (Table 3). Highest potency of ZYBT1 was observed in TMD-8 (1 nmol/L) while that in HBL-1 was the closest follower (12 nmol/L). In MCL and Burkitt's lymphoma, ZYBT1 has shown very weak potency making it unsuitable for these two subtypes. However, in the ABC-DLBCL subgroup itself, U2932 cells (IC_{50} ≈ 1 mol/L) were ~1000-fold resistant than their two close neighbors.

TABLE 2 Activity of ZYBT1 in BTK and other kinases using a kinase profile (IC_{50} values with range found from three independent experiments in 13 selected protein kinases)

Kinase	IC_{50} (μmol/L)
BLK	1.1-2.2
BMX	0.091-0.12
BTK	0.027-0.041
EGFRT790M	4.2-5.7
EGF-R wt	2.3-3.5
ERBB2 wt	1.7-2.3
ERBB4	0.12-0.19
FGR	10-13
FRK	1.3-1.7
HCK	>10
ITK	18-24
JAK3	>10
TEC	0.025-0.038

3.4 | The binding of ZYBT1 to BTK is covalent and irreversible in nature

Since the first FDA approved BTK inhibitor, ibrutinib, works via covalent and irreversible binding, we tested if ZYBT1 also followed a similar mechanism. To that end, we adopted the method described by Honigberg et al[14] Since this paper reported the irreversible binding of PCI-32765 (a.k.a. ibrutinib), we used fluorescence-tagged ibrutinib (IB-BFL) in a THP-1 cell-based binding assay. Analysis of the fluorescent gel showed a fluorescent band at 70 kDa, corresponding to the molecular weight of BTK. The band started appearing at 0.5 μmol/L Ib-BFL and attained saturation at 5 μmol/L and higher concentration (Figure 2A; upper panel). Immunoblotting of the same gel with anti-BTK Ab confirmed the presence of constant levels of total BTK with increasing concentration of IB-BFL (Figure 2A; lower panel). This indicated that IB-BFL binds to BTK and the binding is detectable at and above 0.5 μmol/L. This step was important to find out the concentration of IB-BFL to be used in our corresponding assays. Since 5 μmol/L of Ib-BFL was saturating the binding, we chose 2 μmol/L, a subsaturating concentration for the following experiment.

In order to test whether ibrutinib and ZYBT1 binds to the same site of BTK, we adopted a competition binding assay. In this assay, THP-1 cells were preincubated with increasing concentration of ZYBT1 followed by incubation with 2 μmol/L Ib-BFL. Figure 2B, upper panel clearly showed that Ib-BFL could either replace or occupy free sites, at a ZYBT1 concentration, lower than 5 μmol/L. However, on increasing the concentration of ZYBT1 to 10 μmol/L and above, the Ib-BFL-BTK

TABLE 3 Effect of ZYBT1 on cell proliferation. The IC50 range for cell killing potential (n = 3) were tabulated

Cell line	Type	IC_{50} (nmol/L)
TMD8	ABC-DLBCL	0.78-1.40
HBL-1	ABC-DLBCL	12.0-16.0
U2932	ABC-DLBCL	847-961
SUDHL6	GCB-DLBCL	7120-7850
JEKO	MCL	8740-10 000
Raji	Burkitt's lymphoma	13 200-15 100

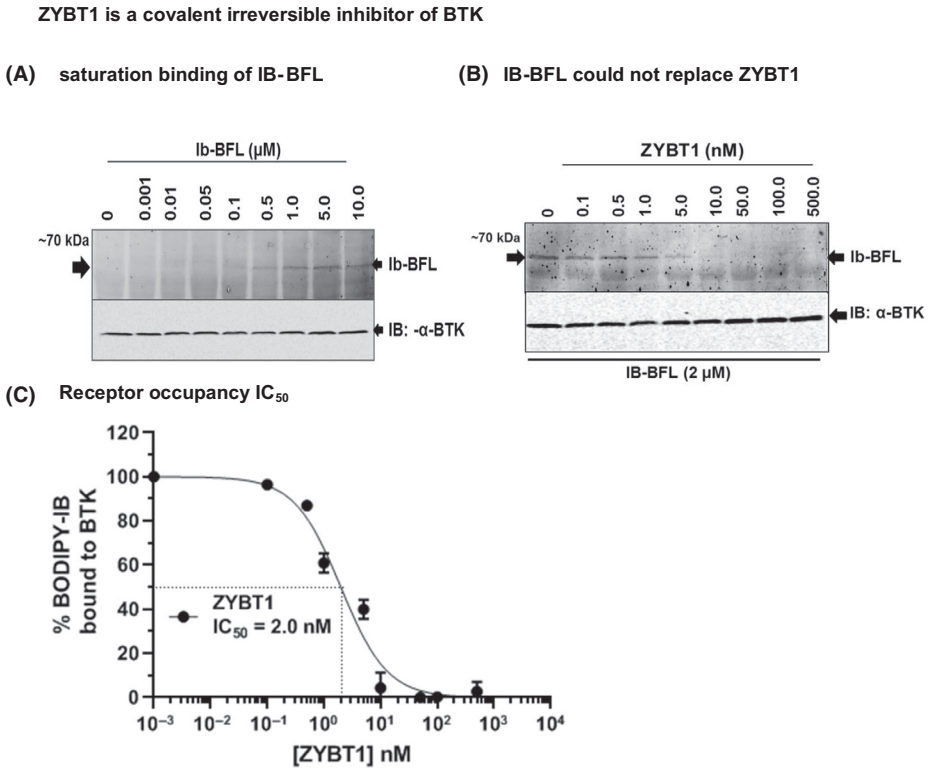

FIGURE 2 ZYBT is an irreversible inhibitor of BTK. (A) Ibrutinib binds to BTK and saturation of binding occurs at 5 μmol/L and above. (B) Ibrutinib failed to replace ZYBT1 from BTK at ZYBT1. (C) ZYBT1 achieved 50 percent receptor (BTK) occupancy at 1 nmol/L. Figures are representative of three independent experiments. Figure 2C represents the densitometric scanning data of the same gel as in Figure 2B and error bars are not incorporated

interaction was no more detectable. Since the levels of BTK did not change (Figure 2B; lower panel), this demonstrated that ZYBT1 binds to the same site as ibrutinib and that the binding is irreversible in nature. A densitometric scanning of the fluorescent bands yielded an IC_{50} of 1 nmol/L for this binding (Figure 2C).

3.5 | The cytotoxic potential of ZYBT1 is retained after washing the drug off

Encouraged by the irreversibility of ZYBT1-BTK binding, we intended to check whether this binding is manifested in its cytotoxic effect. TMD-8 cells were incubated with 25 nmol/L ZYBT1, 25 nmol/L of ibrutinib or 100 nmol/L dasatinib separately for 1 hour and either continued incubation in drug-containing medium or washed off with PBS and fed with fresh drug-free media. As expected, the cell killing was maintained for at least 48 hours both in continuous-drug medium and in the conditions of drug-wash off for ibrutinib and ZYBT1. In fact there was no significant difference between 'wash-off' or 'no wash-off' condition in the cell survival graph (Figure 3A, left and middle panels). On the other hand, dasatinib, a reported reversible binder,[16] failed to exert its effect when washed off and no further cell killing was observed after 24 hours, indicating that the washing protocol that we used was enough to wash out the drug. This clearly showed that an incubation of one hour is enough to maintain the cytotoxicity of ZYBT1 for at least 48 hours.

In order to explain the cytotoxicity, retained after washout of ZYBT1, we reasoned that the ZYBT1-BTK binding is most likely retained for that period. To test the hypothesis, we treated THP-1 cells with 500 nmol/L ZYBT1 for 1 hour and washed it out followed by competition with fluorescent ibrutinib at different time point (0 and 24 hour). Figure 3B left panel clearly demonstrated that ibrutinib failed to displace ZYBT1 even after 24 hours of incubation. Semiquantitative estimation of the band intensity by densitometric scanning demonstrated that more than 95% ZYBT1 was still bound with BTK even after 24 hours (Figure 3B, right panel). Importantly, the phosphorylation of BTK under similar conditions was also completely abolished although there is no change in the total levels of BTK (Figure 3C). The difference between "wash out" and "no wash out" sets in the dasatinib treated cells, but not in ibrutinib and ZYBT1 set validated our wash-out protocol.

3.6 | ZYBT1 inhibited phosphorylation of BTK and PLCγ2

The B-cell signaling pathway involves phosphorylation of BTK and its downstream member PLCγ2. Thus to delineate the mechanism

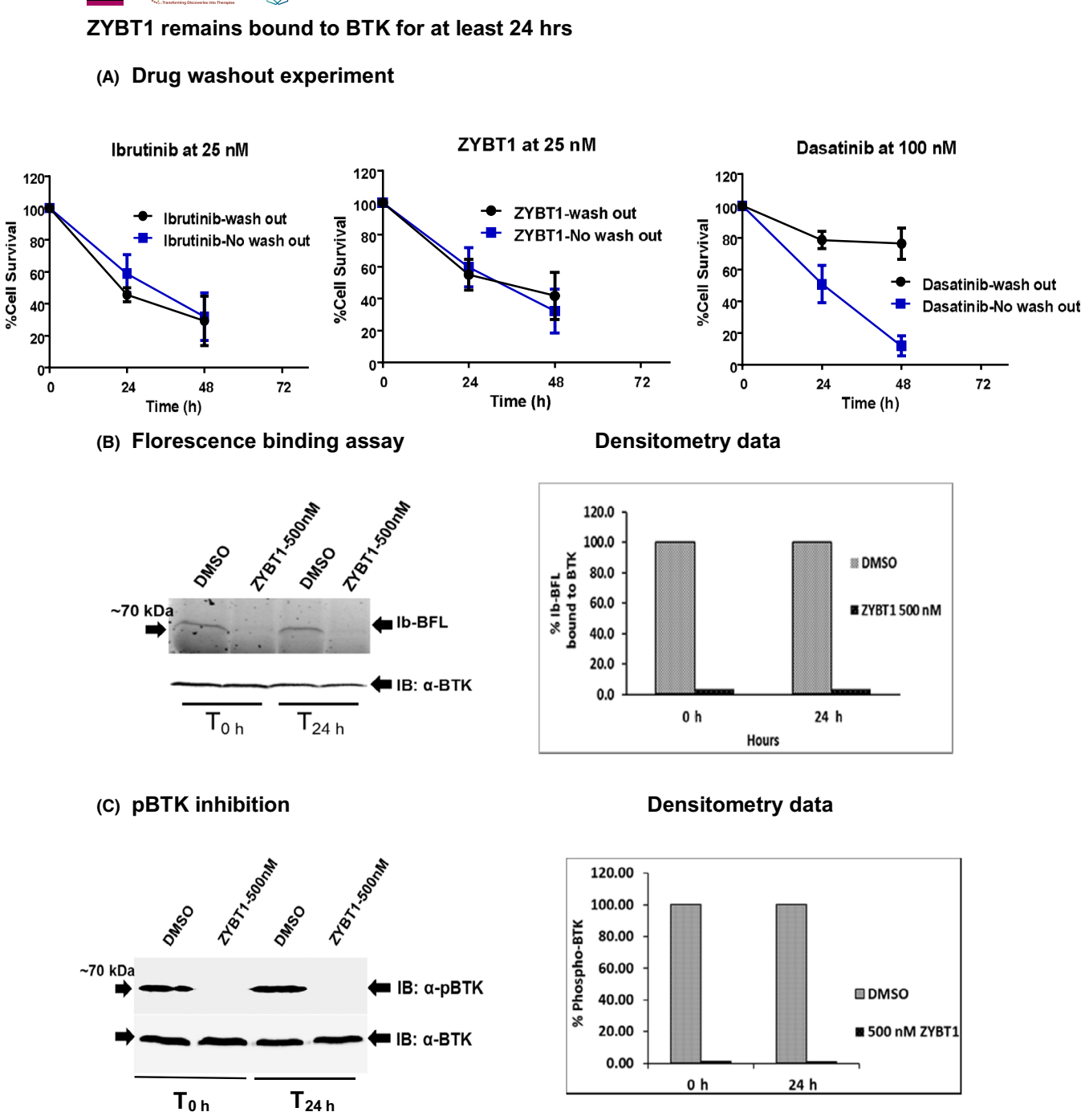

FIGURE 3 ZYBT1 remained bound to BTK for at least 24 hours. (A) Ibrutinib (left) and ZYBT1 (middle) could exert cytotoxicity even 48 hours after washout while dasatinib (right) lost its cell killing potential after washout. (B) ibrutinib could not replace ZYBT1 (500 nmol/L) even after 24 hours of washout (left panel). The densitometric scanning data are presented on the right panel. (C) ZYBT1 inhibited phosphorylation of BTK1 and sustained the inhibition even after 48 hours (left). The graph on the right represents the densitometric scanning of the gel shown in the left panel. Error bars represents SD of triplicate sets. Figures are representative of three independent experiments

of ZYBT1-mediated cytotoxicity further, we opted to check the tyrosine phosphorylation status of these two key players. Treatment of THP-1 cells with increasing concentration of ZYBT1 for one hour showed a dose dependent decrease of phospho-BTK and could completely abrogate phosphorylation of tyrosine 223 at a concentration of 30 nmol/L and higher (Figure 4A). As expected, phosphorylation of tyrosine 1217 in PLCγ2, the substrate of BTK, showed similar downregulation of phosphorylation profile (Figure 4B). The IC_{50} of ZTBT1 for BTK- and PLCγ2-phosphorylation was 2 and 114 nmol/L respectively.

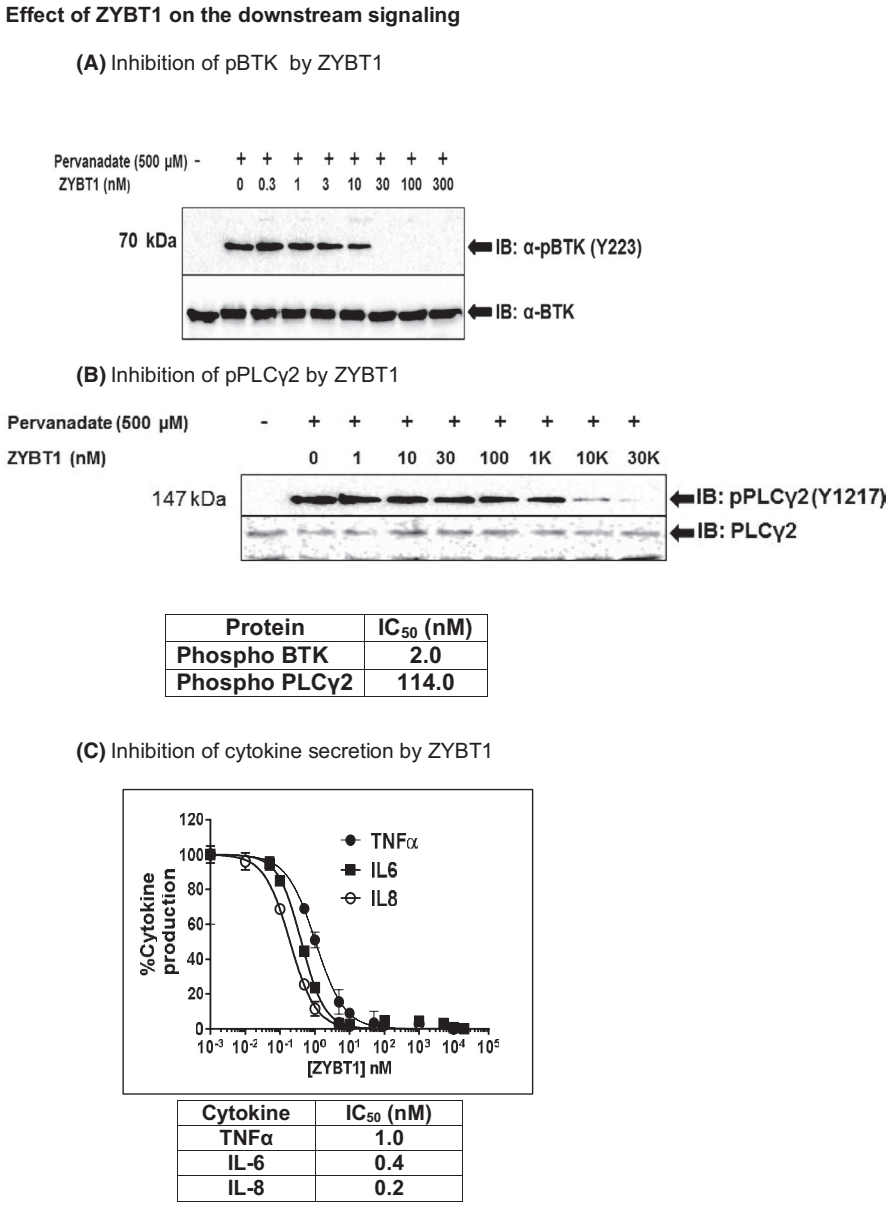

Protein	IC_{50} (nM)
Phospho BTK	2.0
Phospho PLCγ2	114.0

Cytokine	IC_{50} (nM)
TNFα	1.0
IL-6	0.4
IL-8	0.2

FIGURE 4 ZTBT1 inhibited the phosphorylation of (A) BTK (Y223) and (B) PLCγ2 (Y1217). The IC_{50} values are summarized in the following table. (C) ZYBT1 could also suppress the secretion of TNFα (filled circle), IL-6 (square), and IL-8 (open circle) in a cell based assay. The IC_{50} values are shown the attached table. The data presented are representative of three independent experiments

3.7 | ZYBT1 inhibited secretion of TNF-α, IL-6 and IL-8 secretion

Since BTK pathway signaling affects both cell growth and inflammatory pathways, we prompted to check its effect on cytokine signaling. For this purpose, we chose the three major players, TNF-α, IL-6 and IL-8. THP-1 (for TNF-α) and TMD-8 (for IL-6 and IL-8) cells were treated with increasing concentration of ZYBT1 and the levels of TNF-α, IL-6 and IL-8 were measured by ELISA. The secretions of all of them were abolished by ZYBT1 with an IC_{50} of 1.0, 0.4, and 0.2 nmol/L for TNF-α, IL-6 and IL-8 respectively (Figure 4C). This indicated that ZYBT1 also has the potential to inhibit inflammatory responses. It is to be noted that the potency of ZYBT1 for inhibiting cytokine secretion is somewhat higher than that for the inhibition of pBTK. We believe that these differences may be attributed to the difference in assay condition, and the cellular models used.

3.8 | In vitro ADME of ZYBT1

ZYBT1 showed pH dependent solubility. The solubility was found to be 500 μmol/L in an acidic pH of 1.2, and diminished to <2 μmol/L in purified water, and buffers of pH 6.8 and pH 4.5.

ZYBT1 showed low to moderate permeability across Caco2 cells monolayer and found to be a substrate of efflux transporters. The apparent permeability (Papp) was 33 nm/sec with an efflux ratio of 5:1.

ZYBT1 was found to be highly to moderately stable in mouse, rat, dog, and human liver microsomes, while unstable in monkey liver

microsomes. ZYBT1 was metabolized only up to 13% in mouse liver microsomes (mClint: 0.46 mL/min/gm liver) while in rat liver microsomes 55% ZYBT1 was metabolized (mClint: 2.62 mL/min/gm liver). In dog and human liver microsomes ZYBT1 was metabolized upto 18% (mCLint: 0.67 mL/min/gm liver) and 32% (mCLint: 1.28 mL/min/gm liver) respectively. Interestingly, the stability of ZYBT1 was much less in monkey liver microsomes (66% metabolized with mCLlint of 3.49 mL/min/gm liver). ZYBT1 was incubated with recombinant human cytochrome P450 (CYP) enzymes and found to be substrate of CYP3A4.

ZYBT1 showed no inhibition potential (IC_{50}: >30 μmol/L) for CYPs 1A2, 2C19, 2D6, and 3A4 enzymes and was found to be moderate inhibitor of CYPs 2C8 and 2C9 with IC_{50} values of 5.5 and 14.7 μmol/L, respectively, using human liver microsomes.

ZYBT1 showed accepted plasma protein binding ability in rat and human plasma (91.2% and 98.4% in rat and human respectively).

3.9 | Pharmacokinetic parameters of ZYBT1

The pharmacokinetic parameters of ZYBT1 were determined in both mice and rats using both oral and intravenous route of administration. The absolute oral bioavailability of ZYBT1 in mice after administration of 3 mg/kg drug was found to be 47%, with the mean peak plasma concentration (C_{max}) was 703 ng/mL at 0.25 hours (T_{max}), area under the concentration-time curve ($AUC_{0\text{-}inf}$) was 590 ng·h/mL and elimination half-life ($T_{1/2}$) was 0.76 hours. After intravenous administration of ZYBT1 at 1 mg/kg dose administration, total plasma clearance (CL) was found to be 39.5 mL/min/kg, volume of distribution (Vss) was 0.67 L/kg and $T_{1/2}$ was 0.41 hours (Figure 5A).

The PK parameters of ZYBT1 in rats are presented as mean ± SD, n = 4. The absolute oral bioavailability of ZYBT1 in rats (3 mg/mg) was found to be 75%, the peak plasma concentration (Cmax) was 650 ± 222 ng/mL at 0.25 hours (T_{max}), area under the concentration-time curve (AUC 0-inf) was 908 ± 170 ng·h/mL and T1/2 was 2.2 ± 1.3 hours. After intravenous administration of ZYBT1 (1 mg/kg), CL was found to be 36.0 ± 7.8 mL/min/kg, Vss was 0.88 ± 0.12 L/kg and T1/2 was 0.6 ± 0.1 hours (Figure 5B). Besides these studies, we have performed very detailed pharmacokinetics evaluation of ZYBT1, including PK studies at in-vivo efficacy dose in mice (0.2 mg/kg to 30 mg/kg; PO) and rats (3 mg/kg to 30 mg/kg; PO) to get the plasma exposure, associated with efficacy. We have also performed dose linearity PK in rats (10-300 mg/kg; PO) (Table S1). For rat, the exposure to free drug (considering 91% PPB) at efficacy dose was 360 nmol/L which was well above the IC_{50} of ZYBT1 (1 nmol/L).

3.10 | Anti-leukemic activity of ZYBT1 in TMD8 xenograft model

Based on our findings that ZYBT1 reduced tumor growth in our cellular settings, we sought to validate if this cytotoxic effect of ZYBT1 can be translated in-vivo system. To that end, the in vivo antitumor potential of ZYBT1 was assessed in TMD-8 DLBCL xenograft tumor-bearing mice. Mice were treated with 1.5, 3, & 15 mg/kg of ZYBT1, delivered BID, for 20 consecutive days via oral administration. The tumor volume was measured as described above, in the Materials and Method section. ZYBT1 showed a dose dependent tumor growth inhibition 10%, 50%, and 88% respectively (Figure 6A). The growth inhibitory property of ZYBT1 was more prominent after 7 days and onwards. We have also compared the efficacy of ZYBT1 against the two known drugs, ibrutinib and acalabrutinib for its antitumor activities. Our results demonstrated that ZYBT1 had slightly better potency compared to Ibrutinib, while it showed much better efficacy than acalabrutinib (Figures S2 and S3 respectively). It is important to note that ZYBT1 does not have any effect on the body weight of the animal during a 20 day long period of treatment (Figure S4).

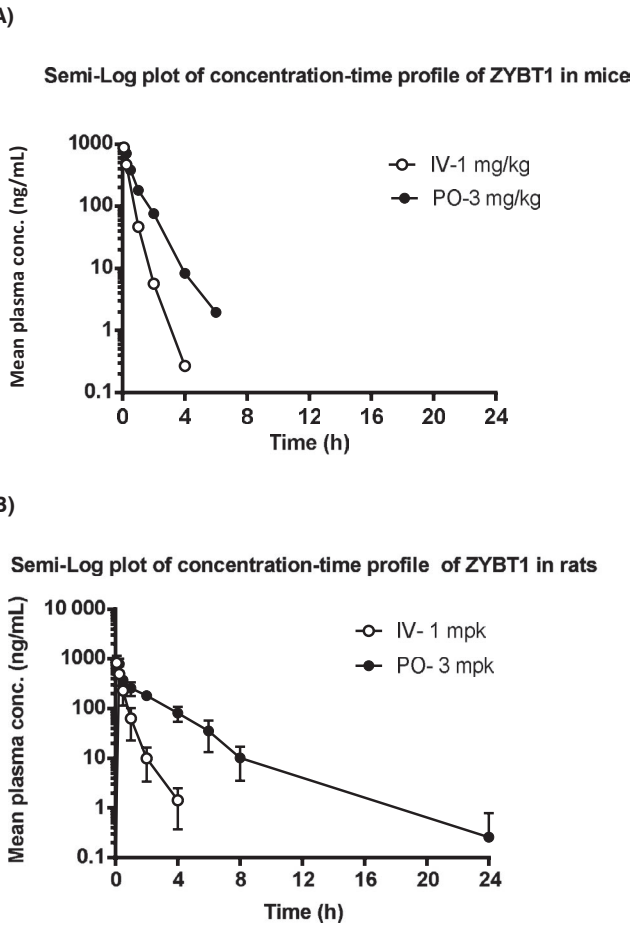

FIGURE 5 PK parameters of ZYBT1. ZYBT was administered via intravenous (IV) or oral route (PO) in either (A) mice or (B) rats. The concentration of ZYBT1 in plasma was measured at indicated time points. Suppression of tumor volume in TMD8 DLBCL xenograft model by ZYBT1. Mice with established tumor reaching around 100 mm^3 were divided into different groups of 10 mice each. Groups were untreated vehicle (triangle) or treated with ZYBT1 [1.5 (square), 3 (triangle) & 15 mg/kg (inverted triangle), BID] for 20 consecutive days. The data represents the mean tumor volume. Error bars represents SEM

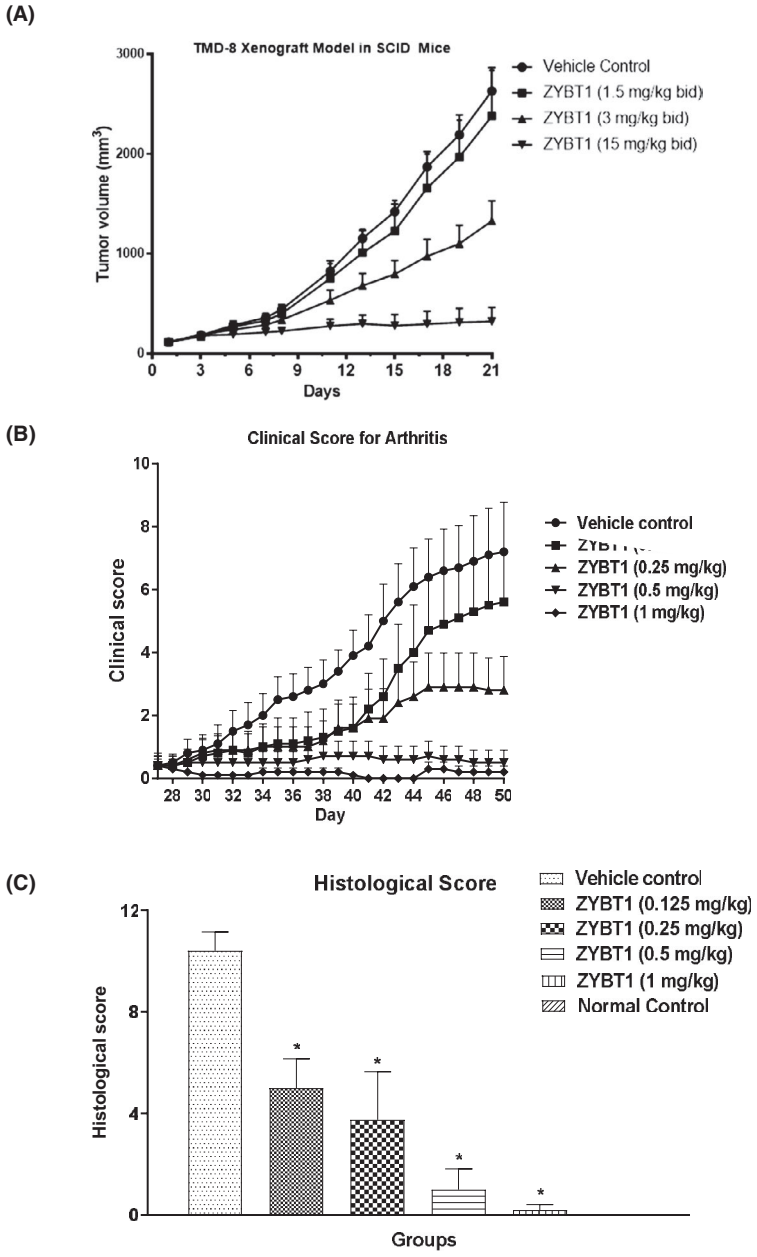

FIGURE 6 Effect of ZYBT1 on in vivo models. (A) Suppression of tumor volume in TMD8 DLBCL xenograft model by ZYBT1. Mice with established tumor reaching around 100 mm^3 were divided into different groups of 10 mice each. Groups were untreated vehicle (triangle) or treated with ZYBT1 [1.5 (square), 3 (triangle) & 15 mg/kg (inverted triangle), BID] for 20 consecutive days. The data represents the mean tumor volume. (B) clinical score and (C) histological score in collagen-induced arthritis (CIA) model. Mice with established CIA were divided into separate groups consisting of 10 mice each. Groups were treated vehicle (circle) or ZYBT1 [0.125(square), 0.25 (triangle), 0.5 (inverted triangle) & 1 mg/kg (diamond), QD] for 20 consecutive days. The data represent the mean arthritic or histological scores. Error bars represent SEM. *$P < .05$ when compared with vehicle control

3.11 | Effects of ZYBT1 in murine CIA model

In the biological framework, BTK is located upstream of NFκB which diverges into both cell proliferation and immunological responses. Accordingly, it is well-documented that BTK-inhibitors may play roles in controlling both these phenomena.[17] Our in vitro data also supported this two-pronged action of BTK. Thus, we opted to check the anti-inflammatory responses of ZYBT1 in in vivo models. To that end, we used collagen-induced arthritis (CIA) model, which has been extensively used in the evaluation of novel therapeutics and reflects many of the clinical and histologic features of human RA. Doses of 0.125, 0.25, 0.5, & 1 mg/kg were administered once daily for 28 days in animals with clear signs of suppression of inflammation. As shown in Figure 6B, treatment with ZYBT1 significantly suppressed progression of the disease. The efficacy was dose related, with 0.25 mg/kg once daily being the lowest, significantly efficacious dose. Improvement in clinical signs of disease were noted as early as 2 days after initiation of dosing, and a dose-dependent reduction of clinical scores compared with vehicle controls—22%, 61%, 93%, and 97%, respectively, was seen at study termination (Figure 6B). Interestingly, while 0.5 mg/kg ZYBT1 caused 93% reduction of clinical score, ibrutinib, at 0.6 mg/kg caused only 40% reduction in same CIA model (Figure S1) indicating superiority of ZYBT1 over ibrutinib. The Inflammation and damage to the paw were also assessed histologically. Treatment with ZYBT1 resulted in a reduction in the damage to the paw based on lower histologic severity scores in the ZYBT1–treated groups compared with the vehicle-treated group. The paws from vehicle-treated control mice had a group mean severity of 10.4, while the groups mean severity scores in the ZYBT1

treated mice were 5, 3.75, 1, and 0.2 at dosages of 0.125, 0.25, 0.5, & 1 mg/kg respectively (Figure 6C). Similar to the xenograft model, we did not observe any body weight change in this model at the end of the study (Figure S5).

3.12 | ZYBT1 Inhibits Inflammation in rat SCW induced arthritis model

To validate the anti-rheumatic potential of ZYBT1 in a second model, we tested the efficacy of ZYBT1 compound in rat SCW, a standard RA model. In the present study, ZYBT1 or vehicle was administered orally to rats twice daily starting on day 14 to 16. As shown in Figure 7A, ZYBT1 treatment resulted in a dose-dependent inhibition of arthritis as indicated by decreased paw volume compared to vehicle treated control rats (Figure 7A). Notably, ZYBT1, at a 75 mg/kg dose, showed complete inhibition of paw volume. ED_{50} of ZYBT1 was found to be 5.6 mg/kg (Figure 7B). RA is a systemic autoimmune disease that causes inflammation not only in the joint but also systemically as demonstrated by increased levels of acute-phase response proteins and other inflammatory markers in the blood. To investigate whether BTK inhibition also modulates serum inflammatory markers, we analyzed IL-6 serum protein. Serum levels of IL-6 was reduced with the treatment in a dose-dependent manner (Figure 7D) and correlated well with paw swelling. SCW injected control animals caused a decrease in body weight. Interestingly, treatment with ZYBT1 restored the body weight in a dose dependent manner and even gained at high doses (Figure 7C).

It is noteworthy, that ZYBT1 in once daily doses in anti-inflammatory models was efficacious, whereas in xenograft models, there was a need to have continuous inhibition of BTK in rapidly proliferating tumor cells. This rational is supported through reports from different groups[18,19] and therefore, a BID dosing regimen was used in these studies.

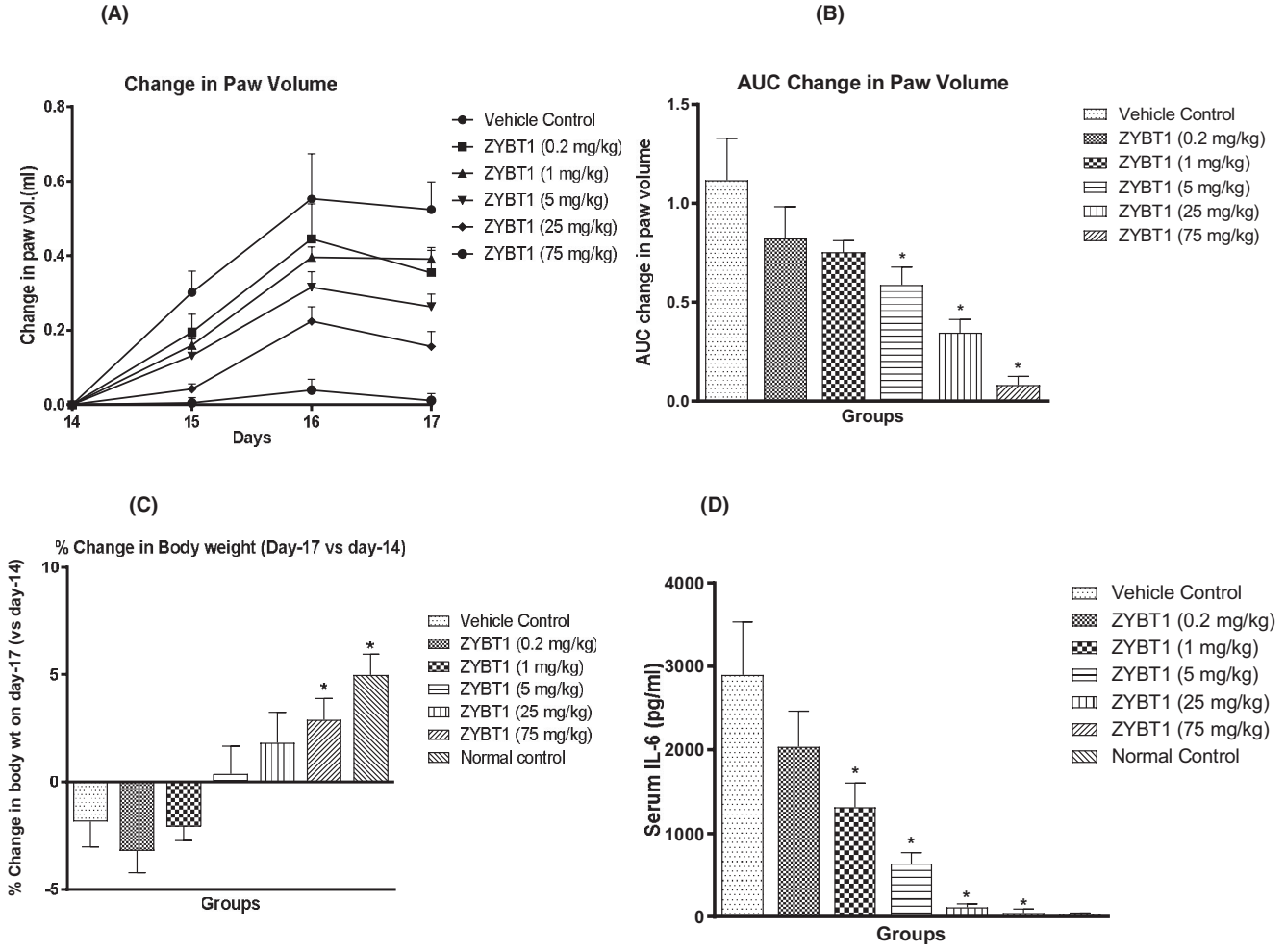

FIGURE 7 Effect of ZYBT1 in the SCW model of arthritis. (A) Changes in paw volume in PG-PS treated Sprague Dawley rats, (B) AUC of change in paw volume, (C) Percentage change in body weight and (D) Effect of ZYBT1 on serum IL-6. Rats were injected with PG-PS into the tibio tarsal joints on day 0. On day 14, PGPS was injected i.v and change in paw volume was monitored from day 14 to 17. Experimental groups were untreated control or treated with ZYBT1 (0.2, 1, 5, 25, 75 mg/kg, QD) from the time of PGPS challenge in SCW (day 14) study. Values are Mean ± SEM $^*P < .05$ when compared with vehicle control

4 | DISCUSSION

Since BTK plays a central role in both blood cancer and autoimmune disorders, developing an inhibitor for BTK has been a very interesting endeavor for researchers. In this manuscript, we report the preclinical profiling of ZYBT1, a potent, specific, and irreversible inhibitor of BTK. ZYBT1 inhibited BTK in a cell free enzymatic assay with an IC_{50} of 1 nmol/L which is comparable to the reported IC_{50} of ibrutinib (0.5 nmol/L).[14] In our laboratory, the IC_{50} of ibrutinib was found to be in the similar range (data not shown). Furthermore, the low nmol/L Ki of ZYBT1 (14 nmol/L) also indicated a strong binding between ZYBT1 and BTK. Ibrutinib and acalabrutinib are the two leading BTK inhibitors that are approved by FDA. Since both of these two acts via covalent modification of Cys481, we performed same sets of experiments as published by Honigberg et al[14] Our result clearly indicated that ZYBT1 is following a similar irreversible mechanism for inhibiting BTK. Since the mechanism of ZYBT1-mediated inhibition involved an irreversible binding, the use of Cheng-Prusoff Equation [20] to interpret the Ki value was not expected to add any further value.

However, the detailed mechanistic aspects of ZYBT1–BTK interaction are not well-understood. So is the importance of C481 in the irreversible and/or covalent mechanism of BTK inhibition. To delineate these aspects, detailed crystallographic and enzymatic studies are warranted. Presently, we are aiming to answer these questions using recombinant BTK and the findings will be discussed in another manuscript.

Recently, cases of ibrutinib-resistance have also been reported. For example, a CLL patient developed resistance to ibrutinib at a relatively high dose of 840 mg per day.[21] Detailed sequencing of the DNA sample from this patient revealed a C481S mutation in the kinase domain of BTK.[14] This resistance might be a manifestation of the C481S mutation in BTK that disrupts the irreversible binding of ibrutinib.[22] Therefore a potent inhibitor, against BTK C481S is needed to overcome ibrutinib resistance. Interestingly, ZYBT1 inhibited BTK (C481S) with an IC_{50} of 14 nmol/L while ibrutinib showed a dwarfed potency for the mutant BTK (IC_{50} = 1 μmol/L).[21] This suggested that ZYBT1 might have better outcome in patients carrying C481S mutant. We are presently checking if this inhibitory potency of ZYBT1 for mutant BTK can be translated in cell based system. Other BTK inhibitors namely, ACP-196, ONO/GS-4050, and BGB-3111 have shown appreciable activity for the mutant BTK.[23] Furthermore, mutations occurring in PLCγ2 (R665W and L845F) have also been reported to impart resistance to ibrutinib,[21] suggesting that newer strategies are needed to combat these and other upcoming ibrutinib-resistance mechanisms.

As mentioned earlier, designing specific kinase inhibitor has always been a challenge due to the homology among the ATP-binding domains of different kinases. For example, besides BTK, ibrutinib inhibits EGFR, TEC and ITK. In our kinase profiling assay, ZYBT1 showed selectivity for BTK and TEC only (IC_{50} are 27 and 38 nmol/L respectively).

Furthermore, we tested its cytotoxic potential using a battery of cell lines representing various subtypes of leukemia namely ABC-DLBCL, GCB-DLBCL, MCL, U2932, and Burkitt's lymphoma. ZYBT1 showed extremely potent cytotoxic potential with IC_{50} ranging from 1 and 12 nmol/L in ABC-DLBCL cell lines with the exception of U2932 (IC_{50} = 961 nmol/L). The high potency of ZYBT1 for TMD-8 and HBL-1 might be due to the presence of wild-type CARD11 while, the lower potency of ZYBT1 for U2932 cell line is probably attributed to the TNFAIP3 mutation or the higher PI-3-Kinase-ATK activity that confers resistance to BCR-mediated cell killing pathways.[24-26] It is important to note that U2932 cell line is also resistant to ibrutinib mediated cytotoxicity.[27-29] ZYBT1 has shown micromolar potency in cell lines from GCB-DLBCL, MCL and Burkitt's lymphoma subtypes. These cell lines contain hyperactive PI3K/AKT/mTOR/MCL1 pathway that may play a compensatory role.[30]

Encouraged by the fact that ibrutinib and ZYBT1 both inhibit BTK, and that the Ki and IC_{50} of ZYBT1 for BTK were different, we opted to check if ZYBT1 binds to BTK in an irreversible manner. It was also important to check if ibrutinib and ZYBT1 bind to the same site of BTK. Since ibrutinib failed to bind BTK when concentration of ZYBT1 was 5 μmol/L or more, we concluded that ZYBT1 binds to BTK in an irreversible manner and that ibrutinib and ZYBT1 bind to the same site of BTK. Concomitantly, ZYBT1 maintained its cytotoxic potential even after 48 hours of wash out in the cell killing experiments. It is worth noting that dasatinib, a reversible inhibitor,[16] completely lost its cytotoxic potential under similar condition. Whether the irreversible binding may interfere with the normal course of proteasome-mediated turnover of BTK is not known at this point. It is also possible that the irreversible binding may give rise to peptide fragments that are not degraded and thus elicit some unwanted immunogenic response. These possibilities need to be comprehensively investigated.

From the mechanistic point of view, ZYBT1 inhibited tyrosine phosphorylation of both BTK and its downstream player PLCγ2. The potential for the inhibition of the latter is although a little bit less. One possible reason for this is the higher levels of expression of PLCγ2 compared to BTK in THP-1 cells (data not shown).

Since BTK plays a central role in inflammatory responses, we expected that ZYBT1 may inhibit these pathways as well. Indeed, ZYBT1 inhibited the secretion of TNF-α, IL-6 and IL-8, with IC_{50} of 1, 0.4, and 0.2 nmol/L respectively. This finding opens the possibility of testing ZYBT1 in auto-immune disorders. However, inhibition of disease-specific cytokines by ZYBT1 is warranted before assigning this molecule for any particular auto-immune disorders.

Given the chemical structure of ZYBT1 and the pharmacokinetic properties of the predecessor ibrutinib,[31,32] it was important to characterize and understand both in vitro and in vivo pharmacokinetic properties of ZYBT1. We have evaluated pharmacokinetic properties of ZYBT1 in mice, rat, dog, and nonhuman primate by oral and intravenous-bolus route, though only mice and rat pharmacokinetic properties of ZYBT1 have been discussed here in correlation with in-vivo efficacy data. Pharmacokinetics of ZYBT1 was evaluated at efficacy dose in mice (0.2-15 mg/kg) and rats (3-30 mg/kg) to get plasma exposure associated with efficacy. The C_{max} of the

free ZYBT1 for both cases were found to be above the IC_{50} of BTK. Ascending single dose linearity pharmacokinetics was performed in rats (10-300 mg/kg) and dogs (5-300 mg/kg).

ZYBT1 showed extreme pH dependence in its solubility. Acidic environment maximized its solubility, directly correlating with quick absorption observed in both rats and mice after oral dosing. Due to a higher efflux ratio, it is expected that higher doses of ZYBT1 may saturate efflux pumps. However, it is unlikely to happen owing to the solubility limitations of ZYBT1 in the small intestinal pH environment. Therefore, it appears that high efflux ratio may be inconsequential if the majority of oral absorption of ZYBT1 occurs in the stomach facilitated by greater solubility of the drug in the acidic pH. To underscore this point, at the oral dose of 3 mg/kg of ZYBT1, the absolute bioavailability was impressive in both preclinical species evaluated. ZYBT1 displayed a fair volume of distribution which may bode well for the cancer indications or auto immune disorders in the sense that it may need to be dosed less frequently. The moderate clearance observed for ZYBT1 in both species suggested that drug is unlikely to accumulate significantly after multiple daily oral doses. The somewhat longer $T_{1/2}$ value for oral vs intravenous dosing was suggestive of a possible flip-flop pharmacokinetics, which further supported the reduced solubility of ZYBT1 as it transits from stomach to small/large intestine. Although moderately stable in human liver microsomes, the incubation of ZYBT1 with human recombinant CYP3A4 showed that ZYBT1 was likely metabolized by this enzymatic pathway and that a CYP3A4 inhibitor may increase the exposure of ZYBT1 (unpublished data). Since our CYP inhibition studies showed that ZYBT1 was not a perpetrator for the inhibition of several important CYP enzymes such as CYP3A4, CYP1A2, CYP2C19, and CYP2D6 (IC_{50} > 30 µmol/L), it showed moderate inhibition of CYPs 2C8 and 2C9 (IC_{50} 5–15 µmol/L). Therefore, the clinical development of ZYBT1 may need to address any drug-drug pharmacokinetic interaction liability. Overall, ZYBT1 showed more than satisfactory in vitro and in vivo pharmacokinetic properties to merit further development.

Considering, BTK's role in both cancer and autoimmune diseases, we checked the efficacy of ZYBT1 in in vivo models for both. Since the cytotoxic potential of ZYBT1 was maximum for TMD-8 cell line (Table 3), we chose this cell line for our xenograft model. ZYBT1 showed a dose dependent reduction of tumor growth when administered orally, confirming its promise as an anti-cancer drug. Similarly, we tested the anti-inflammatory properties of ZYBT1 in a collagen induced arthritis model and streptococcal cell wall (SCW) model and almost complete remission was found only after 20 days of once daily treatment. These in vivo data are in corroboration with our in vitro experiments and is predictive of usability of ZYBT1 for arthritis.

Interestingly, the in vivo potency of ZYBT1 for secretion of IL-6 also closely matched its efficacy dose (Figure 7D) indicating that the mechanism of inhibition of arthritic symptoms involved secretion of IL-6. Importantly, the body weight decrease caused by SCW, was restored with ZYBT1 treatment indicating remission of arthritic symptoms. Among the other BTK inhibitors, BMS-986142 did not inhibit BTK completely in murine CIA and collagen antibody-induced arthritis (CAIA). Correspondingly, a combination of standard anti-arthritic treatment such as methotrexate, TNFα-antagonist or the murine form of CTLA4-Ig along with the BMS compound was more effective,[33] whereas ZYBT1 as a mono therapeutic agent could alleviate the RA symptoms which might be attributed to its ability to inhibit IL-6 secretion completely in both our in-vitro and in-vivo assays. Ibrutinib has also been shown to have similar anti-arthritic activity with a comparable IC_{50} for IL-6 inhibition (3.9 nmol/L) in in-vitro assays and comparable ED_{50} of 2.6 mg/kg/day.[34] The in-vitro potency of ZYBT1 to inhibit IL-6 secretion was similar to ibrutinib (0.5 and 0.4 nmol/L respectively). In fact, in an in-vivo situation, 0.6 mg/kg ZYBT1 furnished comparable efficacy as 3 mg/kg Ibrutinib in arthritis model. In xenograft model, efficacy of ZYBT1 and ibrutinib was comparable (Figure 6A and Figure S1).

Ibrutinib has been shown to cause several adverse effects that may include diarrhea, fatigue, arthralgia, neutropenia, anemia, and others.[35] Importantly, ZYBT1 did not show any change in hematological and biochemical profile, clinical signs and body weight in our toxicological studies in rats up to 300 mg/kg dose (unpublished observation). The safer profile of ZYBT1 may be attributed to its superior specificity for BTK.

All these data taken together, especially the potential of inhibiting C481S mutant BTK and its irreversible binding makes a strong point in favor of using ZYBT1 as an anti-cancer and/or anti-arthritic therapy.

CONFLICT OF INTEREST

We hereby declare that none of the authors have any conflict of interest to disclose.

AUTHORS CONTRIBUTION

Participated in Research designing: Ghoshdastidar, Chatterjee, Mahapatra, Bandyopadhyay, Giri, Srinivas, Bahekar, R Sharma, Desai, Jain. Overall Supervision: R Sharma, Desai, Jain. Conducted experiments: A Patel, H Patel, Thakkar, Bhayani, Dinesh Patel, M Sharma, Singh, Gupta, N Patel, Dipam Patel. Wrote the manuscript: Bandyopadhyay. Study Director: Pankaj Patel.

ORCID

Krishnarup Ghoshdastidar https://orcid.org/0000-0002-1443-2854
Nuggehally R. Srinivas https://orcid.org/0000-0002-5768-1332
Debdutta Bandyopadhyay https://orcid.org/0000-0001-9073-6289

REFERENCES

1. Nogai H, Dörken B, Lenz G. Pathogenesis of non-Hodgkin's lymphoma. *J Clin Oncol*. 2011;29:1803-1811. https://doi.org/10.1200/JCO.2010.33.3252
2. Xia B, Qu F, Yuan T, Zhang Y. Targeting Bruton's tyrosine kinase signaling as an emerging therapeutic agent of B-cell malignancies (Review). *Oncol Lett*. 2015;10:3339–3344. https://doi.org/10.3892/ol.2015.3802

3. de Weers M, Mensink RGJ, Kraakman MEM, Schuurman RKB, Hendriks RW. Mutation analysis of the Bruton's tyrosine kinase gene in X-linked agammaglobulinemia: identification of a mutation which affects the same codon as is altered in immunodeficient xid mice. *Hum Mol Genet*. 1994;3:161-166. https://doi.org/10.1093/hmg/3.1.161
4. Hendriks RW, Yuvaraj S, Kil LP. Targeting Bruton's tyrosine kinase in B cell malignancies. *Nat Rev Cancer*. 2014;14:219-232. https://doi.org/10.1038/nrc3702
5. Edwards JCW, Cambridge G. Prospects for B-cell-targeted therapy in autoimmune disease. *Rheumatology*. 2005;44:151-156. https://doi.org/10.1093/rheumatology/keh446
6. Edwards JCW, Cambridge G. B-cell targeting in rheumatoid arthritis and other autoimmune diseases. *Nat Rev Immunol*. 2006;6:394-403. https://doi.org/10.1038/nri1838
7. Lv J, Wu J, He F, Qu Y, Zhang Q, Yu C. Development of Bruton's tyrosine kinase inhibitors for rheumatoid arthritis. *Curr Med Chem*. 2019;25:5847-5859. https://doi.org/10.2174/0929867325666180316121951
8. Hata D, Kawakami Y, Inagaki N, et al. Involvement of Bruton's tyrosine kinase in FcεRI-dependent mast cell degranulation and cytokine production. *J Exp Med*. 1998;187:1235-1247. https://doi.org/10.1084/jem.187.8.1235
9. Ren LI, Campbell A, Fang H, et al. Analysis of the effects of the Bruton's tyrosine kinase (Btk) inhibitor ibrutinib on monocyte Fcγ receptor (FcγR) function. *J Biol Chem*. 2016;291:3043-3052. https://doi.org/10.1074/jbc.M115.687251
10. Weber ANR, Bittner Z, Liu X, Dang T-M, Radsak MP, Brunner C. Bruton's tyrosine kinase: an emerging key player in innate immunity. *Front Immunol*. 2017;8:1454-1460. https://doi.org/10.3389/fimmu.2017.01454
11. Desai R, Bahekar R, Patel D, Shah K. Heterocyclic compounds. 2015. WO/2015/132799
12. Bahekar RH, Jadav PA, Goswami AD, et al. An efficient and scalable synthesis of tert -butyl (3a R,6a S)-5-oxohexahydrocyclo penta[c]pyrrole-2(1 H)-carboxylate: a pharmacologically important intermediate. *Org Process Res Dev*. 2017;21:266-272. https://doi.org/10.1021/acs.oprd.6b00399
13. Evans EK, Tester R, Aslanian S, et al. Inhibition of Btk with CC-292 provides early pharmacodynamic assessment of activity in mice and humans. *J Pharmacol Exp Ther*. 2013;346:219-228. https://doi.org/10.1124/jpet.113.203489
14. Honigberg LA, Smith AM, Sirisawad M, et al. The Bruton tyrosine kinase inhibitor PCI-32765 blocks B-cell activation and is efficacious in models of autoimmune disease and B-cell malignancy. *Proc Natl Acad Sci*. 2010;107:13075-13080. https://doi.org/10.1073/pnas.1004594107
15. Scales HE, Ierna M, Smith KM, et al. Assessment of murine collagen-induced arthritis by longitudinal non-invasive duplexed molecular optical imaging. *Rheumatology*. 2016;55:564-572. https://doi.org/10.1093/rheumatology/kev361
16. Bradshaw JM, McFarland JM, Paavilainen VO, et al. Prolonged and tunable residence time using reversible covalent kinase inhibitors. *Nat Chem Biol*. 2015;11:525-531. https://doi.org/10.1038/nchembio.1817
17. Shinners NP, Carlesso G, Castro I, et al. Bruton's tyrosine kinase mediates NF-kappa B activation and B cell survival by B cell-activating factor receptor of the TNF-R family. *J Immunol*. 2007;179:3872-3880. http://www.ncbi.nlm.nih.gov/pubmed/17785824
18. Woyach JA, Bojnik E, Ruppert AS, et al. Bruton's tyrosine kinase (BTK) function is important to the development and expansion of chronic lymphocytic leukemia (CLL). *Blood*. 2014;123:1207–1213. https://doi.org/10.1182/blood-2013-07-515361
19. Hutcheson J, Vanarsa K, Bashmakov A, et al. Modulating proximal cell signaling by targeting Btk ameliorates humoral autoimmunity and end-organ disease in murine lupus. *Arthritis Res Ther*. 2012;14:R243. https://doi.org/10.1186/ar4086
20. Yung-Chi C, Prusoff WH. Relationship between the inhibition constant (KI) and the concentration of inhibitor which causes 50 per cent inhibition (I50) of an enzymatic reaction. *Biochem Pharmacol*. 1973;22:3099-3108. https://doi.org/10.1016/0006-2952(73)90196-2
21. Woyach JA, Furman RR, Liu T-M, et al. Resistance mechanisms for the Bruton's tyrosine kinase inhibitor ibrutinib. *N Engl J Med*. 2014;370:2286-2294. https://doi.org/10.1056/NEJMoa1400029
22. Buhimschi AD, Armstrong HA, Toure M, et al. Targeting the C481S ibrutinib-resistance mutation in Bruton's tyrosine kinase using PROTAC-mediated degradation. *Biochemistry*. 2018;57:3564-3575. https://doi.org/10.1021/acs.biochem.8b00391
23. Wu J, Liu C, Tsui ST, Liu D. Second-generation inhibitors of Bruton tyrosine kinase. *J Hematol Oncol*. 2016;9:1-7. https://doi.org/10.1186/s13045-016-0313-y
24. Kloo B, Nagel D, Pfeifer M, et al. Critical role of PI3K signaling for NF-κB-dependent survival in a subset of activated B-cell-like diffuse large B-cell lymphoma cells. *Proc Natl Acad Sci USA*. 2011;108:272–277. https://doi.org/10.1073/pnas.1008969108
25. Davis RE, Ngo VN, Lenz G, et al. Chronic active B-cell-receptor signalling in diffuse large B-cell lymphoma. *Nature*. 2010;463:88–92. https://doi.org/10.1038/nature08638
26. Erdmann T, Klener P, Lynch JT, et al. Sensitivity to PI3K and AKT inhibitors is mediated by divergent molecular mechanisms in subtypes of DLBCL. *Blood*. 2017;130:310–322. https://doi.org/10.1182/blood-2016-12-758599
27. Campbell V, Thompson R, Villegas V, et al. The potent PI3K-δ, γ inhibitor IPI-145 exhibits differential activity in diffuse large B-cell lymphoma (DLBCL) cell lines. *Blood*. 2013;122:1832.
28. Naylor TL, Tang H, Ratsch BA, et al. Protein kinase C inhibitor sotrastaurin selectively inhibits the growth of CD79 mutant diffuse large B-cell lymphomas. *Cancer Res*. 2011;71:2643-2653. https://doi.org/10.1158/0008-5472.CAN-10-2525
29. Paul J, Soujon M, Wengner AM, et al. Simultaneous inhibition of PI3Kδ and PI3Kα induces ABC-DLBCL regression by blocking BCR-dependent and -independent activation of NF-κB and AKT. *Cancer Cell*. 2017;31:64-78. https://doi.org/10.1016/j.ccell.2016.12.003
30. Ezell SA, Wang S, Bihani T, et al. Differential regulation of mTOR signaling determines sensitivity to AKT inhibition in diffuse large B cell lymphoma. *Oncotarget*. 2016;7:9163-9174. https://doi.org/10.18632/oncotarget.7036
31. de Zwart L, Snoeys J, De Jong J, Sukbuntherng J, Mannaert E, Monshouwer M. Ibrutinib dosing strategies based on interaction potential of CYP3A4 perpetrators using physiologically based pharmacokinetic modeling. *Clin Pharmacol Ther*. 2016;100:548-557. https://doi.org/10.1002/cpt.419
32. Scheers E, Leclercq L, de Jong J, et al. Absorption, metabolism, and excretion of oral 14C radiolabeled ibrutinib: an open-label, phase i, single-dose study in healthy men. *Drug Metab Dispos*. 2014;43:289-297. https://doi.org/10.1124/dmd.114.060061
33. Gillooly KM, Pulicicchio C, Pattoli MA, et al. Bruton's tyrosine kinase inhibitor BMS-986142 in experimental models of rheumatoid arthritis enhances efficacy of agents representing clinical standard-of-care. *PLOS One*. 2017;12:e0181782. https://doi.org/10.1371/journal.pone.0181782
34. Chang BY, Huang M, Francesco M, et al. The Bruton tyrosine kinase inhibitor PCI-32765 ameliorates autoimmune arthritis by inhibition of multiple effector cells. *Arthritis Res Ther*. 2011;13:R115. https://doi.org/10.1186/ar3400
35. De Weerdt I, Koopmans SM, Kater AP, Van Gelder M. Incidence and management of toxicity associated with ibrutinib and idelalisib:

a practical approach. *Haematologica*. 2017;102:1629–1639. https://doi.org/10.3324/haematol.2017.164103

SUPPORTING INFORMATION

Additional supporting information may be found online in the Supporting Information section.

How to cite this article: Ghoshdastidar K, Patel H, Bhayani H, et al. ZYBT1, a potent, irreversible Bruton's Tyrosine Kinase (BTK) inhibitor that inhibits the C481S BTK with profound efficacy against arthritis and cancer. *Pharmacol Res Perspect*. 2020;e00565. https://doi.org/10.1002/prp2.565